DOI: 10.1007/s12541-013-0180-1

Model Reference Adaptive Sliding Mode Control for Three Dimensional Overhead Cranes

Le Anh Tuan[1], Soon-Geul Lee[2,#], Luong Cong Nho[3], and Dong Han Kim[4]

1 Research and Development Center, Duy Tan University, Da Nang city, Vietnam
2 Department of Mechanical Engineering, Kyung Hee University, 1 Seocheon-dong, Giheung-gu, Yongin-si, Gyeonggi-do, 449-701
3 Vietnam Maritime University, Hai Phong city, Vietnam
4 Department of Electronics and Radio Engineering, Kyung Hee University, 1 Seocheon-dong, Giheung-gu, Yongin-si, Gyeonggi-do, 449-701
Corresponding Author / E-mail: sglee@khu.ac.kr, TEL: +82-31-2012506, FAX: +82-31-2021204

KEYWORDS: Adaptation mechanism, Lyapunov stability, Overhead cranes, Sliding mode control

An overhead crane transfers the payloads of various volumes and weights depending on the each operation case. The friction factors characterized by damped coefficients can be changed in connection with operating environment. This study develops an adaptive version of sliding mode controller for the overhead cranes without priori information of system parameters composed of cargo mass and damped aspects. The proposed controller simultaneously executes five duties consisted of tracking the trolley and bridge, hoisting the cargo, keeping the payload swings small during the transport process, and absolutely suppressing the cargo vibrations at destination of trolley and bridge. Both simulation and experiment results indicate that the adaptive robust controller asymptotically stabilizes all crane system responses.

Manuscript received: July 11, 2012 / Accepted: May 28, 2013

1. Introduction

Overhead cranes are widely used for handling materials in the industrial factories. For increasing the productivity, the cranes nowadays are required in high-speed operation that easily leads to the large cargo vibrations without good control strategies. This causes the inaccurate motion of crane, makes the unsafe situation in the operation zone, and damages the crane itself.

Up to now, many control techniques have been applied for crane control design from classical methods such as linear control,[1,2] nonlinear strategy,[3-5] optimal control[6] to modern approaches such as command shaping,[7,8] fuzzy logic,[9,10] and neural network.[11,12]

Let us review the previous articles related to robust control technique called Sliding Mode Control (SMC). The general theory of SMC for a class of under-actuated systems was introduced by Lee,[13] developed by Ashrafiuon,[14] and completed by Sankaranarayanan.[15] After that, a series of control crane papers using SMC was published. Karkoub[16] introduced a variable structure controller of crane system in conjunction with a state feedback control law and a μ-synthesis control scheme. Bartolini[17] proposed a simple control structure based on second-order sliding modes for payload-cart system with the constant length of cable. Two SMC schemes[18] of overhead cranes, a PI based controller and a linear observer based time varying feedback scheme, were constructed by Bartolini. To control concurrently the cargo swing and trolley motion, a SMC controller was formed by Lee.[19] This controller was derived from the analysis of sliding surface stability. The sliding surface was defined by linearly combining all state errors. Almutrairi[20] developed the SMC scheme of Lee[19] for 3D crane system. Furthermore, the observer was designed to eliminate the velocities of system outputs. These velocity components were used in SMC scheme as a feedback states. Recently, Ngo[21] discussed a SMC controller for payload anti-sway of container crane. Only the simulation results were shown in this study.

Adaptive control approaches of crane systems can be found in several papers. Using self-turning method, Hua[22] discussed a nonlinear control scheme incorporating parameter adaptive mechanism for 2D overhead crane with the constant length of cable. A developed version of paper[22] was given by Yang[23] in which an adaptive controller for 3D overhead crane was designed without needing any information of crane system parameters. Teo[24] addressed the other adaptive control law for controlling the motion of the overall gantry system without considering the cargo anti-swing control. The adaptive controller was formulated with a priori minimal information assumed of the crane model. Cho[25] proposed the adaptive controller with perturbation consisted of two

components: nominal PD control and corrective one. In study,[26] iterative learning strategy was applied to design a kinematic coupling-based trajectory controller for overhead crane. A motion planning based adaptive control law for overhead crane with constant cable length was proposed by Fang.[27] Three papers, respectively presented by Omar,[28] Giua,[29] and Corriga,[30] applied the gain-scheduling approach for controlling the tower and gantry cranes based on linear crane dynamics. Mizumoto[31] digitally designed a multi-rate adaptive output feedback controller for experimental cart-crane system. Based on a distributed mathematical model, Ngo[32] provided an adaptive scheme using boundary control technique for container crane system.

Combined approaches in crane control problems have received a lot of interests from researchers. Several authors[33,34] integrated the adaptive control technique into SMC controller design of under-actuated systems. Ngo[35] investigated the adaptive SMC controller for container crane in which the switching gain of SMC scheme was considered as a time-varying parameter. A combination of fuzzy logic technique and SMC applied for overhead crane was designed by Liu[36] based on linear mathematical model. With the simplest crane model having constant length cable, an adaptive fuzzy SMC control was presented by Park[37] for cargo anti-swing and trolley tracking.

Our paper analyses and designs the nonlinear controller for 3D overhead cranes based on robust and adaptive control techniques. Let us point out the difference and the improvement of this study compared with the previous papers reviewed above:

The SMC controllers of papers[16-21] guarantee the system robustness. However, these controllers require knowing all crane system parameters. In practice, many crane parameters are not clearly known since they are varied depending on operating crane condition. The recent study improves and upgrades the SMC controllers of papers[16-21] by integrating the adaptation mechanism into SMC structures. By this way, the adaptive SMC controller of this study does not need the information of uncertain crane parameters since the adaptation mechanism automatically estimate the above-mentioned parameters. In principle, this adaptive robust controller is superior to SMC controllers of previous studies[16-21] in dealing with uncertainties. The proposed controller has below two strong points.

(i) Robustness behavior: the controller keeps the system responses consistently in spite of wide variation of system parameters.

(ii) Learning attributes: the controller improves its performance as adaptation goes on. It does not require any priori knowledge of unclear system parameters.

The articles[22-37] studied on control cranes using various kinds of adaptive control techniques from self-turning control,[22,23] corrective nonlinear feedback,[25] iterative learning,[26] adaptive planning control,[27] gain-scheduling,[28-30] multi-rate sampling method,[31] boundary adaptive control,[32] time-varying switching gain based adaptive SMC method[35] to fuzzy based adaptive approach.[36,37] Dissimilar to the above-mentioned papers,[22-37] we still pursue adaptation based SMC controller design but in the other research direction. We apply the adaptive control technique called Model-Reference Adaptive System (MRAS) approach to design the parameter estimating mechanism then integrate it into the SMC loop to become the completed adaptive robust controller.

The objective and the structure of this proposed algorithm are different from those of Ngo's study.[35] His controller is applied to a single input system that had two outputs, meanwhile, the proposed controller is used to a complete multi-input and multi-output system that as three inputs and five outputs. Ngo[35] considered switched gain k of SMC as time-varying gain and proposed an estimator to determine a proper switched gain so as to reduce the system chattering. Dissimilarly, the control algorithm in this paper is proposed to handle the case where four system parameters, those are the payload mass and three friction coefficients, are variable. Parameters adaptation mechanism is designed to estimate four above-mentioned parameters and then integrated into SMC.

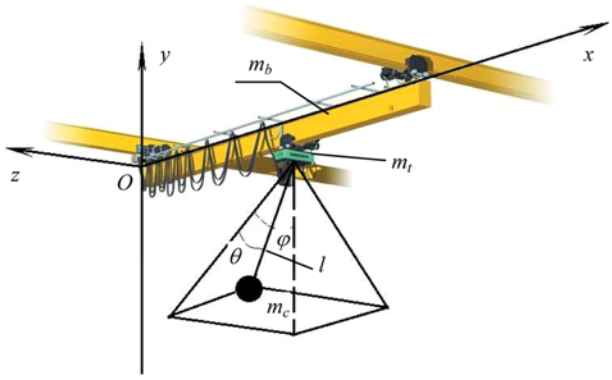

Fig. 1 Physical model of a 3D overhead crane

The efforts of the proposed controllers consisted of bridge travelling, trolley moving, and payload lifting forces are used for controlling five system outputs composed of bridge movement, trolley displacement, cable length, and two cargo swing angles. The controller design mainly comprises synthesizing the SMC scheme and adaptation mechanism. First, based on the stability of sliding surface, a conventional SMC law can be applied to the case that one knows the upper or lower limit values of system parameters. Then, this control law is converted to adaptive form in which the controller parameters are replaced by estimated specifications corresponding to plant parameters. After that, an adaptation mechanism is constructed to adjust the unknown parameters of controller so that the tracking errors converge to zeros. The system stability is investigated using Lyapunov theory. The high qualities of controller are verified by not only numerically simulating but also experimentally studying with the laboratory crane system.

This paper is organized with five sections. The 3D overhead crane dynamics is constituted in section 2. Adaptive robust control design is represented in section 3 composed of proposing an adaptive SMC law, constructing an adaptation parameter mechanism, and analyzing the system stability. Section 4 implements both numerical simulation and experiment study with real-time crane system. Finally, some conclusions and suggestions are mentioned in section 5.

2. System Modeling

The crane system is physically modeled as on Fig. 1. The bridge is a distributed beam whose mass m_b is focused on the bridge center. m_l denotes the equivalent mass of hoist mechanism, m_t and m_c are masses of trolley and cargo, respectively. The overhead crane has five degrees

of freedom corresponding to five generalized coordinates: $x(t)$ is trolley displacement, $z(t)$ indicates bridge movement along Oz axis, and the payload position is described by three generalized coordinates (l, θ, φ). Hence, the positions of system masses are characterized by $\mathbf{q} = [z\ x\ l\ \varphi\ \theta]^T$. The frictions of wire ropes, trolley, and bridge motions are linearly characterized by damped coefficients b_r, b_t, and b_b, respectively. The control signals u_b, u_t, and u_l respectively indicate the driving forces of bridge, trolley, and cargo lifting motions.

Based on Lagrange's equation, the fully nonlinear equations describing the physical behaviors of crane system are obtained as follows

$$\begin{pmatrix} (m_t+m_b+m_c)\ddot{z}+m_c\sin\varphi\cos\theta\ddot{l}+m_c l\cos\varphi\cos\theta\ddot{\varphi} \\ -m_c l\sin\varphi\sin\theta\ddot{\theta}+b_b\dot{z}+2m_c\cos\varphi\cos\theta\dot{l}\dot{\varphi} \\ -2m_c\sin\varphi\sin\theta\dot{l}\dot{\theta}-2m_c l\cos\varphi\sin\theta\dot{\varphi}\dot{\theta} \\ -m_c l\sin\varphi\cos\theta\dot{\varphi}^2-m_c l\sin\varphi\cos\theta\dot{\theta}^2 \end{pmatrix} = u_b, \quad (1)$$

$$\begin{pmatrix} (m_t+m_c)\ddot{x}+m_c\sin\theta\ddot{l}+m_c l\cos\theta\ddot{\theta} \\ +b_t\dot{x}+2m_c\cos\theta\dot{l}\dot{\theta}-m_c l\sin\theta\dot{\theta}^2 \end{pmatrix} = u_t, \quad (2)$$

$$\begin{pmatrix} (m_t+m_c)\ddot{l}+m_c\sin\theta\ddot{x}+m_c\sin\varphi\cos\theta\ddot{z} \\ +b_r\dot{l}+m_c l\dot{\theta}^2-m_c l\cos^2\theta\dot{\varphi}^2-m_c g\cos\varphi\cos\theta \end{pmatrix} = u_t, \quad (3)$$

$$\begin{pmatrix} m_c l\cos\varphi\cos\theta\ddot{z}+m_c l^2\cos^2\theta\ddot{\varphi} \\ +2m_c l\cos^2\theta\dot{l}\dot{\varphi}-2m_c l^2\cos\theta\sin\theta\dot{\varphi}\dot{\theta}+m_c g l\sin\varphi\cos\theta \end{pmatrix} = 0, \quad (4)$$

$$\begin{pmatrix} m_c l\cos\theta\ddot{x}-m_c l\sin\varphi\sin\theta\ddot{z}+m_c l^2\ddot{\theta} \\ +2m_c l\dot{l}\dot{\theta}+m_c l^2\cos\theta\sin\theta\dot{\varphi}^2+m_c g l\cos\varphi\sin\theta \end{pmatrix} = 0, \quad (5)$$

which can be represented in the matrix form as

$$\mathbf{M(q)}\ddot{\mathbf{q}}+\mathbf{B}\dot{\mathbf{q}}+\mathbf{C(q,\dot{q})}\dot{\mathbf{q}}+\mathbf{G(q)}=\mathbf{F}, \quad (6)$$

where, $\mathbf{M(q)} = \mathbf{M^T(q)}$ is symmetric mass matrix. $\mathbf{B}$ denotes damped coefficient matrix. $\mathbf{C(q,\dot{q})}$ is Coriolis and centrifugal matrix. $\mathbf{G(q)}$ is called a gravity vector. $\mathbf{F}$ denotes a vector of control forces. These matrixes and vectors are determined as the below formulas:

$$\mathbf{q}=\begin{bmatrix} z \\ x \\ l \\ \varphi \\ \theta \end{bmatrix}, \mathbf{B}=\begin{bmatrix} b_b & 0 & 0 & 0 & 0 \\ 0 & b_t & 0 & 0 & 0 \\ 0 & 0 & b_r & 0 & 0 \\ 0 & 0 & 0 & 0 & 0 \\ 0 & 0 & 0 & 0 & 0 \end{bmatrix}, \mathbf{C(q,\dot{q})}=\begin{bmatrix} 0 & 0 & c_{13} & c_{14} & c_{15} \\ 0 & 0 & c_{23} & 0 & c_{25} \\ 0 & 0 & 0 & c_{34} & c_{35} \\ 0 & 0 & c_{43} & c_{44} & c_{45} \\ 0 & 0 & c_{53} & c_{54} & c_{55} \end{bmatrix},$$

$$\mathbf{M(q)}=\begin{bmatrix} m_{11} & 0 & m_{13} & m_{14} & m_{15} \\ 0 & m_{22} & m_{23} & 0 & m_{25} \\ m_{31} & m_{32} & m_{33} & 0 & 0 \\ m_{41} & 0 & 0 & m_{44} & 0 \\ m_{51} & m_{52} & 0 & 0 & m_{55} \end{bmatrix}, \mathbf{G(q)}=\begin{bmatrix} 0 \\ 0 \\ g_3 \\ g_4 \\ g_5 \end{bmatrix}, \mathbf{F}=\begin{bmatrix} u_b \\ u_t \\ u_l \\ 0 \\ 0 \end{bmatrix}.$$

The coefficients of $\mathbf{M(q)}$ matrix are given by

$$m_{11}=m_t+m_b+m_c, m_{13}=m_{31}=m_c\sin\varphi\cos\theta,$$
$$m_{14}=m_{41}=m_c l\cos\varphi\cos\theta, m_{15}=m_{51}=-m_c l\sin\varphi\sin\theta,$$
$$m_{22}=m_t+m_c, m_{23}=m_{32}=m_c\sin\theta, m_{25}=m_{52}=m_c l\cos\theta,$$
$$m_{33}=m_t+m_c, m_{44}=m_c l^2\cos^2\theta, m_{55}=m_c l^2.$$

The coefficients of $\mathbf{C(q,\dot{q})}$ matrix are determined by

$$c_{13}=m_c\cos\varphi\cos\theta\dot{\varphi}-m_c\sin\varphi\sin\theta\dot{\theta},$$
$$c_{14}=m_c\cos\varphi\cos\theta\dot{l}-m_c l\cos\varphi\cos\theta\dot{\theta}-m_c l\sin\varphi\cos\theta\dot{\varphi},$$
$$c_{15}=-m_c l\cos\varphi\sin\theta\dot{\varphi}-m_c\sin\varphi\sin\theta\dot{l}-m_c l\sin\varphi\cos\theta\dot{\theta},$$
$$c_{23}=m_c\cos\theta\dot{\theta}, c_{25}=m_c\cos\theta\dot{l}-m_c l\sin\theta\dot{\theta},$$
$$c_{34}=-m_c l\cos^2\theta\dot{\varphi}, c_{35}=-m_c l\dot{\theta}, c_{43}=m_c l\cos^2\theta\dot{\varphi},$$
$$c_{44}=m_c l\cos^2\theta\dot{l}-m_c l^2\cos\theta\sin\theta\dot{\theta}, c_{45}=-m_c l^2\cos\theta\sin\theta\dot{\varphi}$$
$$c_{53}=m_c l\dot{\theta}, c_{54}=m_c l^2\cos\theta\sin\theta\dot{\varphi}, c_{55}=m_c l\dot{l}.$$

The nonzero coefficients of $\mathbf{G(q)}$ vector are given by

$$g_3=-m_c g\cos\varphi\cos\theta, g_4=m_c g l\sin\varphi\cos\theta, g_5=m_c g l\cos\varphi\sin\theta.$$

3. Controller Design

The adaptive SMC controller design involves three steps. First, a conventional control law is designed based on the stability of sliding surface. Second, since payload mass m_c, the friction factors b_b, b_t, b_r are unknown parameters, the above-mentioned control scheme is linearly parameterized with respect to these parameters. Finally, an adaptation mechanism is proposed to adjust the uncertain parameters of crane system (equivalently, corresponding to controller parameters) that are updated to the controller for stabilizing the system responses. Note that the proposed controller together with adaptation structure must well implement five duties composed of precisely driving bridge and trolley to come to their destinations, hoisting the cargo to achieve the desired length of cable, keeping the cargo swing angles small during the transport process, and absolutely suppressing the payload swings at steady-state.

3.1 Decoupling

3D overhead crane is an under-actuated system in which five system outputs are controlled by three actuators. The mathematical model needs to be separated into actuated and un-actuated systems. For this purpose, we define $\mathbf{q}_a = [z\ x\ l]^T$ for actuated states and $\mathbf{q}_u = [\varphi\ \ \theta]^T$ for un-actuated states. The matrix differential equation (6) can be divided into two equations as follows

$$\begin{pmatrix} \mathbf{M}_{11}(\mathbf{q})\ddot{\mathbf{q}}_a+\mathbf{M}_{12}(\mathbf{q})\ddot{\mathbf{q}}_u+\mathbf{B}_{11}\dot{\mathbf{q}}_a \\ +\mathbf{C}_{11}(\mathbf{q},\dot{\mathbf{q}})\dot{\mathbf{q}}_a+\mathbf{C}_{12}(\mathbf{q},\dot{\mathbf{q}})\dot{\mathbf{q}}_u+\mathbf{G}_1(\mathbf{q}) \end{pmatrix} = \mathbf{U}, \quad (7)$$

$$\begin{pmatrix} \mathbf{M}_{21}(\mathbf{q})\ddot{\mathbf{q}}_a+\mathbf{M}_{22}(\mathbf{q})\ddot{\mathbf{q}}_u+\mathbf{C}_{21}(\mathbf{q},\dot{\mathbf{q}})\dot{\mathbf{q}}_a \\ +\mathbf{C}_{22}(\mathbf{q},\dot{\mathbf{q}})\dot{\mathbf{q}}_u+\mathbf{G}_2(\mathbf{q}) \end{pmatrix} = \mathbf{0}, \quad (8)$$

where,

$$\mathbf{M}_{11}(\mathbf{q})=\begin{bmatrix} m_{11} & 0 & m_{13} \\ 0 & m_{22} & m_{23} \\ m_{31} & m_{32} & m_{33} \end{bmatrix},\ \mathbf{M}_{12}(\mathbf{q})=\begin{bmatrix} m_{14} & m_{15} \\ 0 & m_{25} \\ 0 & 0 \end{bmatrix},$$

$$\mathbf{M}_{21}(\mathbf{q})=\begin{bmatrix} m_{41} & 0 & 0 \\ m_{51} & m_{52} & 0 \end{bmatrix},\ \mathbf{M}_{22}(\mathbf{q})=\begin{bmatrix} m_{44} & 0 \\ 0 & m_{55} \end{bmatrix},$$

$$\mathbf{C}_{11}(\mathbf{q},\dot{\mathbf{q}})=\begin{bmatrix} 0 & 0 & c_{13} \\ 0 & 0 & c_{23} \\ 0 & 0 & 0 \end{bmatrix},\ \mathbf{C}_{12}(\mathbf{q},\dot{\mathbf{q}})=\begin{bmatrix} c_{14} & c_{15} \\ 0 & c_{25} \\ c_{34} & c_{35} \end{bmatrix},$$

$$\mathbf{C}_{21}(\mathbf{q},\dot{\mathbf{q}})=\begin{bmatrix} 0 & 0 & c_{43} \\ 0 & 0 & c_{53} \end{bmatrix},\ \mathbf{C}_{22}(\mathbf{q},\dot{\mathbf{q}})=\begin{bmatrix} c_{44} & c_{45} \\ c_{54} & c_{55} \end{bmatrix},$$

$$\mathbf{B}_{11}=\begin{bmatrix} b_b & 0 & 0 \\ 0 & b_t & 0 \\ 0 & 0 & b_r \end{bmatrix},\mathbf{G}_1=\begin{bmatrix} 0 \\ 0 \\ g_3 \end{bmatrix},\mathbf{G}_2=\begin{bmatrix} g_4 \\ g_5 \end{bmatrix},\mathbf{U}=\begin{bmatrix} u_b \\ u_t \\ u_l \end{bmatrix}.$$

Matrix $\mathbf{M}_{22}(\mathbf{q})$ is positive definite. The un-actuated states $\mathbf{q}_u$ is received from Equation (8) as

$$\ddot{\mathbf{q}}_{\mathrm{u}}=-\mathbf{M}_{22}^{-1}(\mathbf{q})\begin{pmatrix}\mathbf{M}_{21}(\mathbf{q})\ddot{\mathbf{q}}_a+\mathbf{C}_{21}(\mathbf{q},\dot{\mathbf{q}})\dot{\mathbf{q}}_a \\ +\mathbf{C}_{22}(\mathbf{q},\dot{\mathbf{q}})\dot{\mathbf{q}}_u+\mathbf{G}_2(\mathbf{q})\end{pmatrix}. \tag{9}$$

The cargo swings $\mathbf{q}_u=[\varphi \quad \theta]^{\mathrm{T}}$ is directly concerned with motion properties of trolley, bridge, and cable length. Substituting Equation (9) into (7) and simplifying lead to

$$\overline{\mathbf{M}}(\mathbf{q})\ddot{\mathbf{q}}_a+\overline{\mathbf{C}}_1(\mathbf{q},\dot{\mathbf{q}})\dot{\mathbf{q}}_a+\overline{\mathbf{C}}_2(\mathbf{q},\dot{\mathbf{q}})\dot{\mathbf{q}}_u+\overline{\mathbf{G}}(\mathbf{q})=\mathbf{U}, \tag{10}$$

where,

$$\overline{\mathbf{M}}(\mathbf{q})=\mathbf{M}_{11}(\mathbf{q})-\mathbf{M}_{12}(\mathbf{q})\mathbf{M}_{22}^{-1}(\mathbf{q})\mathbf{M}_{21}(\mathbf{q}),$$
$$\overline{\mathbf{C}}_1(\mathbf{q},\dot{\mathbf{q}})=\mathbf{B}_{11}+\mathbf{C}_{11}(\mathbf{q},\dot{\mathbf{q}})-\mathbf{M}_{12}(\mathbf{q})\mathbf{M}_{22}^{-1}(\mathbf{q})\mathbf{C}_{21}(\mathbf{q},\dot{\mathbf{q}}),$$
$$\overline{\mathbf{C}}_2(\mathbf{q},\dot{\mathbf{q}})=\mathbf{C}_{12}(\mathbf{q},\dot{\mathbf{q}})-\mathbf{M}_{12}(\mathbf{q})\mathbf{M}_{22}^{-1}(\mathbf{q})\mathbf{C}_{22}(\mathbf{q},\dot{\mathbf{q}}),$$
$$\overline{\mathbf{G}}(\mathbf{q})=\mathbf{G}_1(\mathbf{q})-\mathbf{M}_{12}(\mathbf{q})\mathbf{M}_{22}^{-1}(\mathbf{q})\mathbf{G}_2(\mathbf{q}).$$

After some calculation, the above-mentioned matrices are described as follows

$$\overline{\mathbf{M}}(\mathbf{q})=m_c\begin{bmatrix} \dfrac{m_t+m_b}{m_c}+\sin^2\varphi\cos^2\theta & \dfrac{\sin\varphi\sin 2\theta}{2} & \sin\varphi\cos\theta \\ \dfrac{\sin\varphi\sin 2\theta}{2} & \dfrac{m_t}{m_c}+\sin^2\theta & \sin\theta \\ \sin\varphi\cos\theta & \sin\theta & \dfrac{m_l}{m_c}+1 \end{bmatrix},$$

$$\overline{\mathbf{C}}_1(\mathbf{q},\dot{\mathbf{q}})=\begin{bmatrix} b_b & 0 & 0 \\ 0 & b_t & 0 \\ 0 & 0 & b_r \end{bmatrix},\ \overline{\mathbf{C}}_2(\mathbf{q},\dot{\mathbf{q}})=-m_c l\begin{bmatrix} \sin\varphi\cos^3\theta\dot{\varphi} & \sin\varphi\cos\theta\dot{\theta} \\ \cos^2\theta\sin\theta\dot{\varphi} & \sin\theta\dot{\theta} \\ \cos^2\theta\dot{\varphi} & \dot{\theta} \end{bmatrix},$$

$$\overline{\mathbf{G}}(\mathbf{q})=-m_c g\cos\varphi\cos\theta\begin{bmatrix} \sin\varphi\cos\theta \\ \sin\theta \\ 1 \end{bmatrix}.$$

Mathematical model governed by Equations (9) and (10) will be applied for designing the SMC scheme in the next section.

3.2 Conventional Control Scheme

In the case that all system parameters are clearly known, let us design a nonlinear controller to track the actuated states $\mathbf{q}_a$ to reach desired values $\mathbf{q}_{ad}=[z_d \quad x_d \quad l_d]^T$ and cargo swing angles $\mathbf{q}_u$ approach $\mathbf{q}_{ud}=[0 \quad 0]^T$, asymptotically. The design of control scheme is composed of two phases. First, the sliding surface is chosen in terms of tracking errors of both actuated states and un-actuated one. Second, the control scheme is designed so that all state trajectories are attracted to sliding surface and pushed to the reference values on this surface. Consider the tracking errors

$$\mathbf{e}_a=\mathbf{q}_a-\mathbf{q}_{ad}=[z-z_d \quad x-x_d \quad l-l_d]^T$$

and

$$\mathbf{e}_u=\mathbf{q}_u-\mathbf{q}_{ud}=[\varphi \quad \theta]^T.$$

By linearly combining between position and velocity errors, the sliding surface is defined as

$$\mathbf{s}=[s_1 \ s_2 \ s_3]^T=\dot{\mathbf{e}}_a+\lambda\mathbf{e}_a+\alpha\mathbf{e}_u=\dot{\mathbf{q}}_a+\lambda(\mathbf{q}_a-\mathbf{q}_{ad})+\alpha\mathbf{q}_u \tag{11}$$

where, λ and α are design parameters determined by

$$\lambda=\begin{bmatrix} \lambda_1 & 0 & 0 \\ 0 & \lambda_2 & 0 \\ 0 & 0 & \lambda_3 \end{bmatrix},\ \alpha=\begin{bmatrix} \alpha_1 & 0 \\ 0 & \alpha_2 \\ 0 & 0 \end{bmatrix}.$$

Differentiating the sliding surface $\mathbf{s}$ with respect to time yields

$$\dot{\mathbf{s}}=\ddot{\mathbf{q}}_a+\lambda\dot{\mathbf{q}}_a+\alpha\dot{\mathbf{q}}_u. \tag{12}$$

Let us now create the control input to stabilize the sliding surface. Consider the stable dynamics of switching surface

$$\dot{\mathbf{s}}+\lambda\mathbf{s}=\mathbf{0}. \tag{13}$$

Obviously, the surface $\mathbf{s}$ defined by Equation (13) exponentially converges to $\mathbf{0}$ as $t\to\infty$ for every positive constant matrix λ. Substituting actuated states received from Equation (10) and Equation (12) into sliding surface dynamics (13), one obtains the equivalent control input

$$\begin{aligned}\mathbf{U}_{eq}=&\overline{\mathbf{C}}_1(\mathbf{q},\dot{\mathbf{q}})\dot{\mathbf{q}}_a+\overline{\mathbf{C}}_2(\mathbf{q},\dot{\mathbf{q}})\dot{\mathbf{q}}_u+\overline{\mathbf{G}}(\mathbf{q})\\&-\overline{\mathbf{M}}(\mathbf{q})(2\lambda\dot{\mathbf{q}}_a+\lambda^T\lambda(\mathbf{q}_a-\mathbf{q}_{ad})+\alpha\dot{\mathbf{q}}_u+\lambda\alpha\mathbf{q}_u).\end{aligned} \tag{14}$$

3.3 Adaptation Mechanism

The crane transports many kinds of cargos with the differences in mass m_c and volume. The friction factors (characterized by coefficients b_b, b_t, b_r) can be varied in connection with environment condition of factory. In this case, the plant parameters m_c, b_b, b_t, b_r are not accuracy known. Therefore, they are replaced by estimated parameters $\hat{m}_c,\hat{b}_b,\hat{b}_t,\hat{b}_r$. The "parameters" of controller $\overline{\mathbf{M}}(\mathbf{q}),\overline{\mathbf{C}}_1(\mathbf{q},\dot{\mathbf{q}}),\overline{\mathbf{C}}_2(\mathbf{q},\dot{\mathbf{q}}),\overline{\mathbf{G}}(\mathbf{q})$ now become adjustable parameter matrices as follows

$$\hat{\mathbf{M}}(\mathbf{q}) = \hat{m}_c \begin{bmatrix} \frac{m_t+m_b}{\hat{m}_c} + \sin^2\varphi\cos^2\theta & \frac{\sin\varphi\sin 2\theta}{2} & \sin\varphi\cos\theta \\ \frac{\sin\varphi\sin 2\theta}{2} & \frac{m_t}{\hat{m}_c} + \sin^2\theta & \sin\theta \\ \sin\varphi\cos\theta & \sin\theta & \frac{m_l}{\hat{m}_c} + 1 \end{bmatrix},$$

$$\hat{\mathbf{C}}_1(\mathbf{q},\dot{\mathbf{q}}) = \begin{bmatrix} \hat{b}_b & 0 & 0 \\ 0 & \hat{b}_t & 0 \\ 0 & 0 & \hat{b}_r \end{bmatrix}, \quad \hat{\mathbf{C}}_2(\mathbf{q},\dot{\mathbf{q}}) = -\hat{m}_c l \begin{bmatrix} \sin\varphi\cos^3\theta\dot{\varphi} & \sin\varphi\cos\theta\dot{\theta} \\ \cos^2\theta\sin\theta\dot{\varphi} & \sin\theta\dot{\theta} \\ \cos^2\theta\dot{\varphi} & \dot{\theta} \end{bmatrix},$$

$$\hat{\mathbf{G}}(\mathbf{q}) = -\hat{m}_c g \cos\varphi\cos\theta \begin{bmatrix} \sin\varphi\cos\theta \\ \sin\theta \\ 1 \end{bmatrix}.$$

In case of adaptive control, the conventional control scheme (14) is modified with regard to estimation parameters. The adaptive controller derived from expression (14) has the form of

$$\begin{aligned} \hat{\mathbf{U}} &= \hat{\mathbf{C}}_1(\mathbf{q},\dot{\mathbf{q}})\dot{\mathbf{q}}_a + \hat{\mathbf{C}}_2(\mathbf{q},\dot{\mathbf{q}})\dot{\mathbf{q}}_u + \hat{\mathbf{G}}(\mathbf{q}) \\ &\quad -\hat{\mathbf{M}}(\mathbf{q})(2\lambda\dot{\mathbf{q}}_a + \lambda^T\lambda(\mathbf{q}_a - \mathbf{q}_{ad}) + \alpha\dot{\mathbf{q}}_u + \lambda\alpha\mathbf{q}_u), \end{aligned} \tag{15}$$

where, $\hat{\mathbf{M}}(\mathbf{q}), \hat{\mathbf{C}}_1(\mathbf{q},\dot{\mathbf{q}}), \hat{\mathbf{C}}_2(\mathbf{q},\dot{\mathbf{q}}), \hat{\mathbf{G}}(\mathbf{q})$ (or equivalently, $\hat{m}_c, \hat{b}_b, \hat{b}_t, \hat{b}_r$) are received from the adaptation mechanism which takes charge of updating the parameters for controller.

Inserting adaptive control law (15) into actuated dynamics (10) yields sliding surface model

$$\overline{\mathbf{M}}(\mathbf{q})(\dot{\mathbf{s}} + \lambda\mathbf{s}) = \tilde{\mathbf{M}}(\mathbf{q})\mathbf{q}_{ar} + \tilde{\mathbf{C}}_1(\mathbf{q},\dot{\mathbf{q}})\dot{\mathbf{q}}_a + \tilde{\mathbf{C}}_2(\mathbf{q},\dot{\mathbf{q}})\dot{\mathbf{q}}_u + \tilde{\mathbf{G}}(\mathbf{q}), \tag{16}$$

where, $\mathbf{q}_{ar} = [z_r\ x_r\ l_r]^T = -2\lambda\dot{\mathbf{q}}_a - \lambda^T\lambda(\mathbf{q}_a - \mathbf{q}_{ad}) - \alpha\dot{\mathbf{q}}_u - \lambda\alpha\mathbf{q}_u$ is the vector of "reference position corresponding to desired value $\mathbf{q}_{ad}$. $\tilde{\mathbf{M}}(\mathbf{q}), \tilde{\mathbf{C}}_1(\mathbf{q},\dot{\mathbf{q}}), \tilde{\mathbf{C}}_2(\mathbf{q},\dot{\mathbf{q}})$ and $\tilde{\mathbf{G}}(\mathbf{q})$ indicate the estimation matrices of parameter errors of controller that are respectively determined by

$$\tilde{\mathbf{M}}(\mathbf{q}) = \hat{\mathbf{M}} - \overline{\mathbf{M}} = \tilde{m}_c \begin{bmatrix} \sin^2\varphi\cos^2\theta & \frac{\sin\varphi\sin 2\theta}{2} & \sin\varphi\cos\theta \\ \frac{\sin\varphi\sin 2\theta}{2} & \sin^2\theta & \sin\theta \\ \sin\varphi\cos\theta & \sin\theta & 1 \end{bmatrix},$$

$$\tilde{\mathbf{C}}_1(\mathbf{q},\dot{\mathbf{q}}) = \hat{\mathbf{C}}_1 - \overline{\mathbf{C}}_1 = \begin{bmatrix} \tilde{b}_b & 0 & 0 \\ 0 & \tilde{b}_t & 0 \\ 0 & 0 & \tilde{b}_r \end{bmatrix},$$

$$\tilde{\mathbf{C}}_2(\mathbf{q},\dot{\mathbf{q}}) = \hat{\mathbf{C}}_2 - \overline{\mathbf{C}}_2 = -\tilde{m}_c l \begin{bmatrix} \sin\varphi\cos^3\theta\dot{\varphi} & \sin\varphi\cos\theta\dot{\theta} \\ \cos^2\theta\sin\theta\dot{\varphi} & \sin\theta\dot{\theta} \\ \cos^2\theta\dot{\varphi} & \dot{\theta} \end{bmatrix},$$

$$\tilde{\mathbf{G}}(\mathbf{q}) = \hat{\mathbf{G}} - \overline{\mathbf{G}} = -\tilde{m}_c g\cos\varphi\sin\theta \begin{bmatrix} \sin\varphi\cos\theta \\ \sin\theta \\ 1 \end{bmatrix}.$$

with $\tilde{m}_c = \hat{m}_c - m_c$, $\tilde{b}_b = \hat{b}_b - b_b$, $\tilde{b}_t = \hat{b}_t - b_t$ and $\tilde{b}_r = \hat{b}_r - b_r$ denoting the plant parameter estimation errors.

Based on the form of error dynamics (16), the structure of adaptation mechanism is suggested as follows

$$\hat{m}_c = \gamma_1 \begin{bmatrix} \left(l\sin\varphi\cos^3\theta\dot{\varphi}^2 + l\sin\varphi\cos\theta\dot{\theta}^2 + \frac{g\sin 2\varphi\cos^2\theta}{2} \right) s_1 \\ -\left(-\sin^2\varphi\cos^2\theta z_r - \frac{\sin\varphi\sin 2\theta x_r}{2} - \sin\varphi\cos\theta l_r \right) s_2 \\ -\left(\sin\varphi\cos\theta z_r + \sin\theta x_r + l_r - l\cos^2\theta\dot{\varphi}^2 \right) s_3 \\ -\left(l\dot{\theta}^2 - g\cos\varphi\sin\theta \right) \end{bmatrix}, \tag{17}$$

$$\hat{b}_b = -\gamma_2 \dot{z} s_1, \tag{18}$$

$$\hat{b}_t = -\gamma_3 \dot{x} s_2, \tag{19}$$

$$\hat{b}_r = -\gamma_4 \dot{l} s_3, \tag{20}$$

where z_r, x_r, l_r are respectively written by

$$z_r = -2\lambda_1\dot{z} - \lambda_1^2(z - z_d) - \alpha_1\dot{\varphi} - \lambda_1\alpha_1\varphi, \tag{21}$$

$$x_r = -2\lambda_2\dot{x} - \lambda_2^2(x - x_d) - \alpha_2\dot{\theta} - \lambda_2\alpha_2\theta, \tag{22}$$

$$l_r = -2\lambda_3\dot{l} - \lambda_3^2(l - l_d). \tag{23}$$

Theorem : The adaptive controller (15) together with the adaptation mechanism described by expressions (17)-(23) asymptotically stabilizes the sliding surface defined by equation (12)

Proof : Consider the Lyapunov candidate of the form

$$V = \frac{1}{2}\left(\mathbf{s}^T\overline{\mathbf{M}}(\mathbf{q})\mathbf{s} + \frac{1}{\gamma_1}\tilde{m}_c^2 + \frac{1}{\gamma_2}\tilde{b}_b^2 + \frac{1}{\gamma_3}\tilde{b}_t^2 + \frac{1}{\gamma_4}\tilde{b}_r^2 \right). \tag{24}$$

The derivative of V with respect to time is written by

$$\dot{V} = \mathbf{s}^T\overline{\mathbf{M}}(\mathbf{q})\dot{\mathbf{s}} + \frac{1}{2}\mathbf{s}^T\dot{\overline{\mathbf{M}}}(\mathbf{q})\mathbf{s} + \frac{1}{\gamma_1}\tilde{m}_c\dot{\hat{m}}_c + \frac{1}{\gamma_2}\tilde{b}_b\dot{\hat{b}}_b + \frac{1}{\gamma_3}\tilde{b}_t\dot{\hat{b}}_t + \frac{1}{\gamma_4}\tilde{b}_r\dot{\hat{b}}_r. \tag{25}$$

Inserting expression (16) into (25), one obtains

$$\begin{aligned} \dot{V} &= \mathbf{s}^T\left(\overline{\mathbf{M}}(\mathbf{q})\mathbf{q}_{ar} + \tilde{\mathbf{C}}_1(\mathbf{q},\dot{\mathbf{q}})\dot{\mathbf{q}}_a + \tilde{\mathbf{C}}_2(\mathbf{q},\dot{\mathbf{q}})\dot{\mathbf{q}}_u + \tilde{\mathbf{G}}(\mathbf{q}) + \frac{1}{2}\dot{\overline{\mathbf{M}}}(\mathbf{q})\mathbf{s} \right) \\ &\quad + \frac{1}{\gamma_1}\tilde{m}_c\dot{\hat{m}}_c + \frac{1}{\gamma_2}\tilde{b}_b\dot{\hat{b}}_b + \frac{1}{\gamma_3}\tilde{b}_t\dot{\hat{b}}_t + \frac{1}{\gamma_4}\tilde{b}_r\dot{\hat{b}}_r - \mathbf{s}^T\overline{\mathbf{M}}(\mathbf{q})\lambda\mathbf{s}. \end{aligned} \tag{26}$$

Substituting the adaptation mechanism (17)-(23) into expression (26) yields

$$\dot{V} = -\mathbf{s}^T\overline{\mathbf{M}}(\mathbf{q})\lambda\mathbf{s}. \tag{27}$$

Note that $\overline{\mathbf{M}}(\mathbf{q})$ is a symmetric matrix having $a_{11} = m_t + m_b + m_c\sin^2\varphi\cos^2\theta > 0$ and determinants of upper left sub-matrices of $\overline{\mathbf{M}}(\mathbf{q})$ are

$$\det(\overline{\mathbf{M}}_1(\mathbf{q})) = \left(m_t^2 + m_t m_b + m_t m_c\sin^2\varphi\cos^2\theta + (m_t m_c + m_b m_c)\sin^2\theta \right) > 0,$$

and

$$\det(\overline{\mathbf{M}}(\mathbf{q})) = \left(m_t(m_t + m_c)(m_t + m_b) + m_c m_l(m_t + m_b)\sin^2\theta + m_t m_c m_l\sin^2\varphi\cos^2\theta \right) > 0.$$

Therefore, $\overline{\mathbf{M}}(\mathbf{q})$ is positive definite which leads to $\dot{V} \le 0$ for every positive matrix λ. This implies that $V \le V(0)$, and thus, $\mathbf{s}$, $\tilde{m}_c, \tilde{b}_b, \tilde{b}_t$, and $\tilde{b}_r$ are bounded. Applying Barbalat's lemma,[39] one can easily indicates that $\mathbf{s} \to \mathbf{0}$ as $t \to \infty$. Hence, the sliding surface asymptotically stabilized.

3.4 Adaptive SMC controller

The adaptive control law (15) is used to attract the system states to sliding surface. For keeping the trajectories of outputs on this surface consistently, the switched action should be added to Equation (15). The adaptive sliding mode control scheme is finally obtained as

$$\begin{aligned}\mathbf{U} = {} & \hat{\mathbf{C}}_1(\mathbf{q},\dot{\mathbf{q}})\dot{\mathbf{q}}_a + \hat{\mathbf{C}}_2(\mathbf{q},\dot{\mathbf{q}})\dot{\mathbf{q}}_u + \hat{\mathbf{G}}(\mathbf{q}) \\ & - \hat{\mathbf{M}}(\mathbf{q})(2\lambda\dot{\mathbf{q}}_a + \lambda^T\lambda(\mathbf{q}_a - \mathbf{q}_{ad}) + \alpha\dot{\mathbf{q}}_u + \lambda\alpha\mathbf{q}_u) - \mathbf{K}\,\mathbf{sgn}(\mathbf{s})\end{aligned} \tag{28}$$

with $\mathbf{K} = \mathrm{diag}(K_1, K_2, K_3)$. The equivalent component of controller (28) is used for low frequency control action. Conversely, switched component **sgn**(**s**) corresponds to high frequency control. Normally, the switching control causes the chattering of state trajectory around sliding surface. To reduce this, the sign function should be replaced by a saturation function as

$$\mathrm{sat}(s_i) = \begin{cases} 1 & \text{if } s_i/\varepsilon > 1 \\ s_i/\varepsilon & \text{if } -1 < s_i/\varepsilon < 1 \\ 1 & \text{if } s_i/\varepsilon < -1 \end{cases}, \tag{29}$$

where ε is a constant indicating the thickness of boundary layer.

4. Simulation and Experiment

Let us investigate the crane responses under the action of the adaptive SMC controller (28). The system dynamics (7-8) driven by adaptive robust actuators (28) together with adaptation mechanism (17-23) is numerically simulated. The plant parameters using for simulation involve

$m_t = 5$ kg, $m_b = 7$ kg, $m_l = 2$ kg.

The true values of payload mass and damped coefficients are respectively assumed to be

$m_c = 0.85$ kg, $b_b = 30$ N.s/m, $b_t = 20$ N.s/m, $b_r = 50$ N.s/m.

The control law parameters are chosen as follows

$\lambda_1 = 0.95$, $\lambda_2 = 1.1$, $\lambda_3 = 0.8$, $\alpha_1 = -12$, $\alpha_2 = -14$,

$K_1 = 1.5$, $K_2 = 0.7$, $K_3 = 11$.

The parameters of adaptation mechanism are taken to be

$\gamma_1 = 6$, $\gamma_2 = \gamma_3 = \gamma_4 = 0.5$.

The control input (28) drives the bridge to move to 0.5 m position, the trolley to reach 0.4 m destination, and the cargo to be lifted from 1 m initial cable length to 0.7 m, simultaneously. Assume that the cargo is initially suspended so that the wire rope is perpendicular to ground, $\theta(0) = \varphi(0) = 0^o$. The initial values of estimated plant parameters are chosen to be zeros, $\hat{m}_c(0) = \hat{b}_r(0) = \hat{b}_t(0) = \hat{b}_r(0) = 0$, indicating no priori information of these parameters.

The real-time experiment is also executed with a laboratory crane system depicted in Fig. 2. The overhead crane consists of three DC motors used for driving bridge and trolley, hoisting the cargo. Five incremental encoders measure the bridge movement, the trolley displacement, the cable length, and two payload swing angles. The real-time crane system is controlled by hoist PC based on the MATLAB and SIMULINK environments with xPC Target solution. Two interfacing cards are attached to the target PC for connecting the signals to crane system: The NI PCI 6025E multifunction card is used to send the direction control signals to the motor amplifiers. The NI PCI 6602 card is used for acquiring the pulse signals from the encoders and sending PWM signals to the amplifiers.

The simulation and experiment results are illustrated in Figs. 3-16.

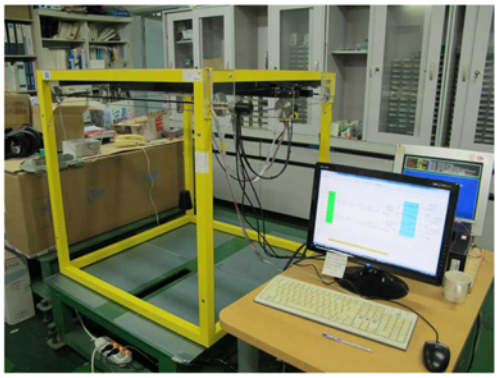

Fig. 2 An overhead crane system for experiment

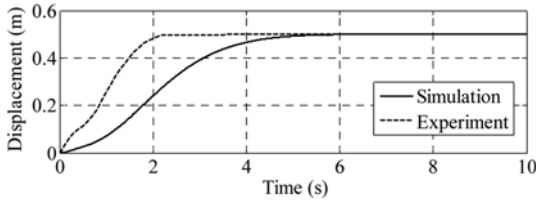

Fig. 3 Bridge motion

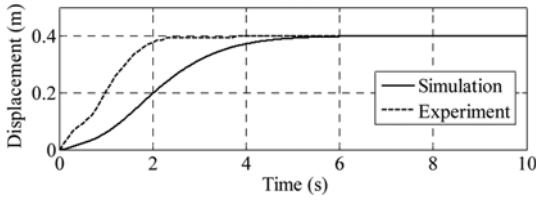

Fig. 4 Trolley motion

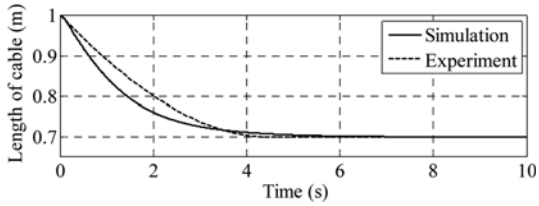

Fig. 5 Cargo lifting motion

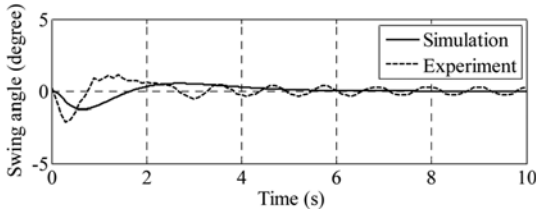

Fig. 6 Cargo swing angle φ

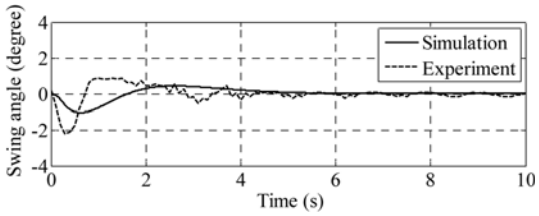

Fig. 7 Cargo swing angle θ

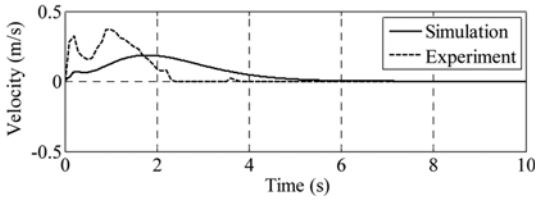

Fig. 8 Bridge velocity

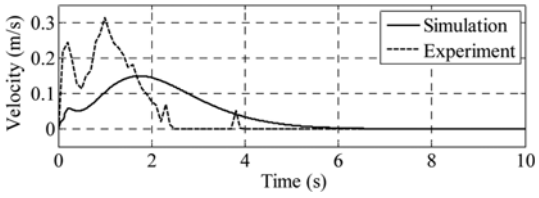

Fig. 9 Trolley velocity

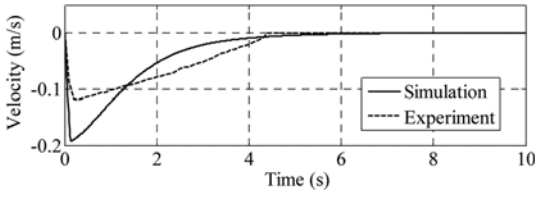

Fig. 10 Cargo lifting velocity

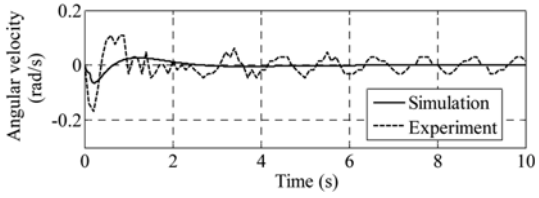

Fig. 11 Cargo swing velocity $\dot{\varphi}$

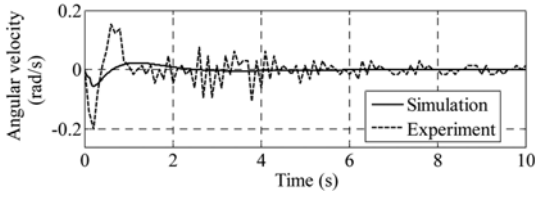

Fig. 12 Cargo swing velocity $\dot{\theta}$

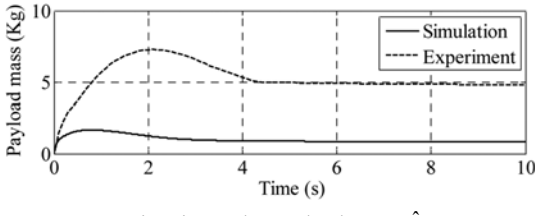

Fig. 13 Parameter estimation – the payload mass $\hat{m}_c$

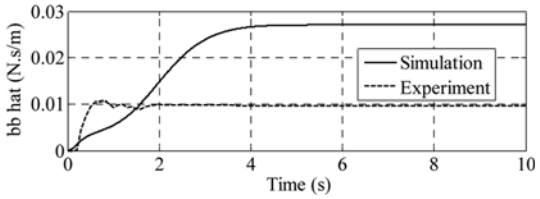

Fig. 14 Parameter estimation – the damping coefficient $\hat{b}_b$

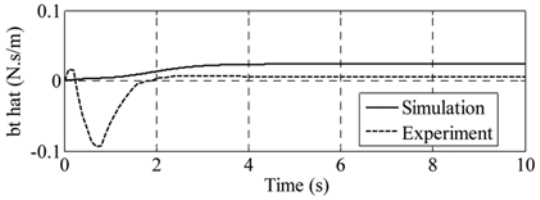

Fig. 15 Parameter estimation – the damping coefficient $\hat{b}_t$

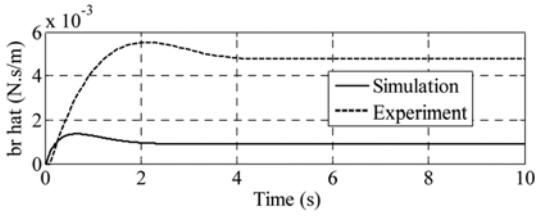

Fig. 16 Parameter estimation – the damping coefficient $\hat{b}_r$

The responses of bridge and trolley motions, cargo lifting motion respectively demonstrated in Figs. 3-5 asymptotically converge to desired destinations. Bridge motion achieves 0.5 m of endpoint within 3.6 seconds for experiment, 5.8 seconds for simulation. Trolley is precisely tracked to reach to 0.4 m position after 3.7 seconds for experiment, 6.1 seconds for simulation. Payload is lifted from 1 m initial cable length to 0.7 m desired length of wire rope after 4.2 seconds for experiment, 6.1 seconds for simulation. The simulated responses are smoother than the experiment ones.

The cargo swing angles with respect to the moving directions of bridge and trolley are respectively depicted in Figs 6 & 7. The cargo vibrations are kept very small during the transfer process that are almost all inconsiderable, $\varphi_{\max} = 1.3^{\circ}$ for simulation and $\varphi_{\max} = 2.1^{\circ}$ for experiment, $\theta_{\max} = 0.9^{\circ}$ for simulation and $\theta_{\max} = 2.2^{\circ}$ for experiment. For the simulation cases, the cargo swings are absolutely eliminated at steady-states. However, the experimental responses still remain the steady-state errors although they are very tiny, $e_{ss} = 0.3^{\circ}$ for φ-trajectory and for θ-response.

The velocities of system responses are plotted in Figs. 8-12. At transient state, the velocities of bridge and trolley motions and cargo lifting displacement are divided into two states corresponding to increasing speed period and decreasing one. We can clearly see from simulated velocities that bridge speeds up during 1.9 initial seconds and speeds down within 3.9 remaining seconds, trolley moves rapidly within 1.8 seconds and slowly during 4.2 remaining seconds, cargo is lifted with growing speed within 0.2 first seconds and with reducing speed within 5.9 remaining seconds.

Figs. 13-16 show the estimation of crane system parameters. Only the estimated payload mass $\hat{m}_c$ of the simulation case converges to the true mass $m_c = 0.85$ kg. The other estimated parameters, $\hat{b}_b, \hat{b}_t$ and $\hat{b}_r$,

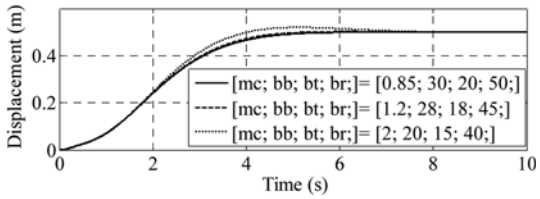

Fig. 17 Bridge motion for various system parameters

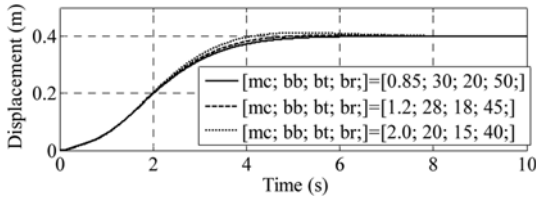

Fig. 18 Trolley motion for various system parameters

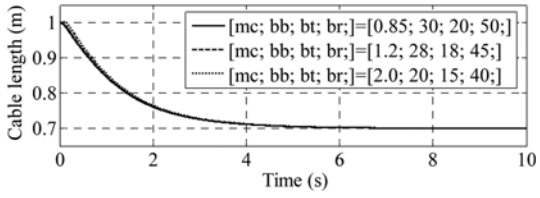

Fig. 19 Cargo lifting motion for various system parameters

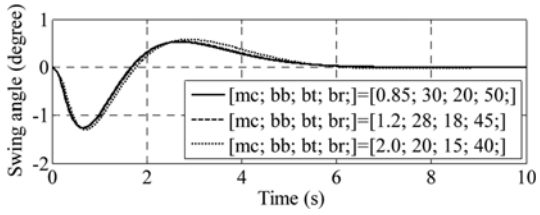

Fig. 20 Cargo swing angle φ for various system parameters

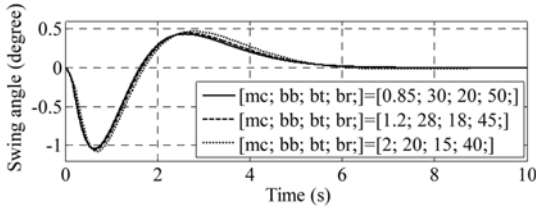

Fig. 21 Cargo swing angle θ for various system parameters

asymptotically reach to specific values that are largely different from the true parameters, b_b, b_t, b_r. This can be explained that the convergences of system outputs can be achieved by many possible values of estimated parameters besides the true parameters. Therefore, the controller does not bother to find out the true parameters.[38] The main objective of the controller is to stabilize asymptotically the system outputs. Hence, the convergence of the estimated plant parameters does not reflect the important meaning of crane control problem.

The system robustness is investigated with several values of parameters [m_c b_b b_t b_r]. Figs. 17-21 show the simulation responses when system parameters [m_c b_b b_t b_r] are varied. All system responses are kept consistently even though there are large variations of system parameters.

5. Conclusions

Using MRAS technique, a novel adaptive robust controller is proposed for 3D overhead cranes in the case that almost all the crane system parameters are not clearly known. The controller is designed for the most complicated operation of crane system in which all crane's mechanism are simultaneously operated consisted of moving the bridge, tracking the trolley, lifting or lowering the cargo, remaining the cargo vibrations in a small boundary, and completely suppressing the cargo swings at steady destination. Both the simulation and experiment study are fully investigated. The achieved results show that the controller works well and all crane system responses are asymptotically stabilized. Integrating the modern techniques, such as fuzzy logic, neural network, to adaptive SMC controllers will be considered in the future works.

ACKNOWLEDGEMENT

This research was supported in part by the IT R&D program of MKE/KEIT (KI10040990, a Development of Communication Technology with UTIS & Vehicle Safety Support Service for Urban Area), by a grant of the SMART Highway Agency from Construction Technology Innovation Program funded by Ministry of Land, Transportation and Maritime Affairs, and by the Technology Innovation Program (No. 10041834) of MKE/KEIT.

REFERENCES

1. Sawodny, O., Aschemann, H., and Lahres, S., "An automated gantry crane as a large workspace robot," Control Engineering Practice, Vol. 10, No. 12, pp. 1323-1338, 2002.

2. Sakawa, Y. and Sano, H., "Nonlinear model and linear robust control of overhead traveling cranes," Nonlinear Analysis, Theory, Methods and Applications, Vol. 30, No. 4, pp. 2197-2207, 1997.

3. Lee, H. H., "A new motion-planning scheme for overhead cranes with high-speed hoisting," ASME Journal of Dynamic Systems, Measurement and Control, Vol. 126, No. 2, pp. 359-364, 2004.

4. Kim, C. S. and Hong, K. S., "Boundary control of container cranes from the perspective of controlling an axially moving string system," International Journal of Control, Automation and Systems, Vol. 7, No. 3, pp. 437-445, 2009.

5. Dongkyoung, C., "Nonlinear Tracking Control of 3-D Overhead Cranes Against the Initial Swing Angle and the Variation of Payload Weight," IEEE Transactions on Control Systems Technology, Vol. 17, No. 4, pp. 876-883, 2009.

6. Wang, Z. and Surgenor, B. W., "A problem with the LQ control of overhead cranes," ASME Journal of Dynamic Systems, Measurement and Control, Vol. 128, No. 2, pp. 436-440, 2006.

7. Sorensen, K. L., Singhose, W., and Dickerson, S., "A controller enabling precise positioning and sway reduction in bridge and

gantry cranes," Control Engineering Practice, Vol. 15, No. 7, pp. 825-837, 2007.

8. Singhose, W., Kim, D., and Kenison, M., "Input shaping control of double-pendulum bridge crane oscillations," Journal of Dynamic Systems, Measurement and Control, Transactions of the ASME, Vol. 130, No. 3, pp. 2008.
9. Chang, C. Y. and Chiang, K. H., "Fuzzy projection control law and its application to the overhead crane," Mechatronics, Vol. 18, No. 10, pp. 607-615, 2008.
10. Chen, Y. J., Wang, W. J., and Chang, C. L., "Guaranteed cost control for an overhead crane with practical constraints: Fuzzy descriptor system approach," Engineering Applications of Artificial Intelligence, Vol. 22, No. 4-5, pp. 639-645, 2009.
11. Suh, J. H., Lee, J. W., Lee, Y. J., and Lee, K. S., "Anti-sway position control of an automated transfer crane based on neural network predictive PID controller," Journal of Mechanical Science and Technology, Vol. 19, No. 2, pp. 505-519, 2005.
12. Yu, W., Moreno-Armendariz, M. A., and Rodriguez, F. O., "Stable adaptive compensation with fuzzy CMAC for an overhead crane," Information Sciences, Vol. 181, No. 21, pp. 4895-4907, 2011.
13. Lee, K., Coates, S., and Coverstone-Carroll, V., "Variable structure control applied to underactuated robots," Robotica, Vol. 15, No. 3, pp. 313-318, 1997.
14. Ashrafiuon, H. and Erwin, R. S., "Sliding mode control of underactuated multibody systems and its application to shape change control," International Journal of Control, Vol. 81, No. 12, pp. 1849-1858, 2008.
15. Sankaranarayanan, V. and Mahindrakar, A. D., "Control of a class of underactuated mechanical systems using sliding modes," IEEE Transactions on Robotics, Vol. 25, No. 2, pp. 459-467, 2009.
16. Karkoub, M. A. and Zribi, M., "Robust control schemes for an overhead crane," Journal of Vibration and Control, Vol. 7, No. 3, pp. 395-416, 2001.
17. Bartolini, G., Pisano, A., and Usai, E., "Second-order sliding-mode control of container cranes," Automatica, Vol. 38, No. 10, pp. 1783-1790, 2002.
18. Bartolini, G., Pisano, A., and Usai, E., "Output-feedback control of container cranes: A Comparative analysis," Asian Journal of Control, Vol. 5, No. 4, pp. 578-593, 2003.
19. Lee, H. H., Liang, Y., and Segura, D., "A Sliding-Mode Antiswing Trajectory Control for Overhead Cranes With High-Speed Load Hoisting," Journal of Dynamic Systems, Measurement, and Control, Vol. 128, No. 4, pp. 842-845, 2006.
20. Almutairi, N. B. and Zribi, M., "Sliding mode control of a three-dimensional overhead crane," JVC/Journal of Vibration and Control, Vol. 15, No. 11, pp. 1679-1730, 2009.
21. Ngo, Q. H. and Hong, K. S., "Sliding-mode antisway control of an offshore container crane," IEEE/ASME Transactions on Mechatronics, Vol. 17, No. 2, pp. 201-209, 2012.
22. Yang, J. H. and Yang, K. S., "Adaptive coupling control for overhead crane systems," Mechatronics, Vol. 17, No. 2-3, pp. 143-152, 2007.
23. Yang, J. and Shen, S., "Novel Approach for Adaptive Tracking Control of a 3-D Overhead Crane System," Journal of Intelligent and Robotic Systems, Vol. 62, No. 1, pp. 59-80, 2011.
24. Teo, C. S., Tan, K. K., Lim, S. Y., Huang, S., and Tay, E. B., "Dynamic modeling and adaptive control of a H-type gantry stage," Mechatronics, Vol. 17, No. 7, pp. 361-367, 2007.
25. Cho, H. C. and Lee, K. S., "Adaptive control and stability analysis of nonlinear crane systems with perturbation," Journal of Mechanical Science and Technology, Vol. 22, No. 6, pp. 1091-1098, 2008.
26. Ning, S., Yongchun, F., Yudong, Z., and Bojun, M., "A Novel Kinematic Coupling-Based Trajectory Planning Method for Overhead Cranes," IEEE/ASME Transactions on Mechatronics, Vol. 17, No. 1, pp. 166-173, 2012.
27. Fang, Y., Ma, B., Wang, P., and Zhang, X., "A motion planning-based adaptive control method for an underactuated crane system," IEEE Transactions on Control Systems Technology, Vol. 20, No. 1, pp. 241-248, 2012.
28. Omar, H. M. and Nayfeh, A. H., "Gain scheduling feedback control of tower cranes with friction compensation," JVC/Journal of Vibration and Control, Vol. 10, No. 2, pp. 269-289, 2004.
29. Corriga, G., Giua, A., and Usai, G., "An implicit gain-scheduling controller for cranes," IEEE Transactions on Control Systems Technology, Vol. 6, No. 1, pp. 15-20, 1998.
30. Giua, A., Sanna, M., and Seatzu, C., "Observer-Controller Design for Three Dimensional Overhead Cranes Using Time-Scaling," Mathematical and Computer Modelling of Dynamical Systems, Vol. 7, No. 1, pp. 77-107, 2001.
31. Mizumoto, I., Chen, T., Ohdaira, S., Kumon, M., and Iwai, Z., "Adaptive output feedback control of general MIMO systems using multirate sampling and its application to a cart-crane system," Automatica, Vol. 43, No. 12, pp. 2077-2085, 2007.
32. Ngo, Q. H., Hong, K. S., and Jung, I. H., "Adaptive control of an axially moving system," Journal of Mechanical Science and Technology, Vol. 23, No. 11, pp. 3071-3078, 2010.
33. Huang, Y. J., Kuo, T. C., and Chang, S. H., "Adaptive Sliding-Mode Control for Nonlinear Systems With Uncertain Parameters," IEEE Transactions on Systems, Man, and Cybernetics, Vol. 38, No. 2, pp. 534-539, 2008.
34. Su, C. Y. and Leung, T. P., "Sliding mode controller with bound estimation for robot manipulators," IEEE Transactions on Robotics and Automation, Vol. 9, No. 2, pp. 208-214, 1993.
35. Ngo, Q. H. and Hong, K. S., "Adaptive sliding mode control of container cranes," IET Control Theory and Applications, Vol. 6, No. 5, pp. 662-668, 2012.

36. Liu, D., Yi, J., Zhao, D., and Wang, W., "Adaptive sliding mode fuzzy control for a two-dimensional overhead crane," Mechatronics, Vol. 15, No. 5, pp. 505-522, 2005.

37. Park, M. S., Chwa, D. K., and Hong, S. K., "Antisway tracking control of overhead cranes with system uncertainty and actuator nonlinearity using an adaptive fuzzy sliding mode control," IEEE Transactions on Industrial Electronics, Vol. 55, No. 11, pp. 3972-3984, 2003.

38. Slotine, J. J. E. and LI, W. A., "Applied Nonlinear Control," Prentice Hall, 1991.

39. Le, T. A., Kim, G. H., Kim, M. Y., and Lee, S. G., "Partial feedback linearization control of overhead cranes with varying cable lengths," Int. J. Precis. Eng. Manuf., Vol. 13, No. 4, pp. 501-507, 2012.

40. Tuan, L. A., Moon, S. C., Lee, W. G., and Lee, S. G., "Adaptive sliding mode control of overhead cranes with varying cable length," Journal of Mechanical Science and Technology, Vol. 27, No. 3, pp. 885-893, 2013.

41. Le, T. A., Dang, V.-H., Ko, D. H., An, T. N., and Lee, S.-G., "Nonlinear controls of a rotating tower crane in conjunction with trolley motion," Proceedings of the Institution of Mechanical Engineers, Part I: Journal of Systems and Control Engineering, Vol. 227, No. 5, pp. 451-460, 2013.

42. Le, A. T. and Lee, S. G., "Sliding Mode Controls of Double-Pendulum Crane Systems," Journal of Mechanical Science and Technology, Nol. 27, No. 6, pp. 1863-1873, 2013.

43. Tuan, L. A., Kim, G. H., and Lee, S. G., "Partial Feedback Linearization Control of the three dimensional overhead crane," IEEE Ineternational Conference on Automation Science and Engineering, pp. 1198-1203, 2012.